

Seed-Based Region Growing (SBRG) vs Adaptive Network-Based Inference System (ANFIS) vs Fuzzy c-Means (FCM): Brain Abnormalities Segmentation

Shafaf Ibrahim, Noor Elaiza Abdul Khalid, and Mazani Manaf

Abstract—Segmentation of Magnetic Resonance Imaging (MRI) images is the most challenging problems in medical imaging. This paper compares the performances of Seed-Based Region Growing (SBRG), Adaptive Network-Based Fuzzy Inference System (ANFIS) and Fuzzy c-Means (FCM) in brain abnormalities segmentation. Controlled experimental data is used, which designed in such a way that prior knowledge of the size of the abnormalities are known. This is done by cutting various sizes of abnormalities and pasting it onto normal brain tissues. The normal tissues or the background are divided into three different categories. The segmentation is done with fifty seven data of each category. The knowledge of the size of the abnormalities by the number of pixels are then compared with segmentation results of three techniques proposed. It was proven that the ANFIS returns the best segmentation performances in light abnormalities, whereas the SBRG on the other hand performed well in dark abnormalities segmentation.

Keywords—Seed-Based Region Growing (SBRG), Adaptive Network-Based Fuzzy Inference System (ANFIS), Fuzzy c-Means (FCM), Brain segmentation.

I. INTRODUCTION

SEGMENTATION is the labeling of objects in image data. It has been a crucial stage in many medical imaging processing tasks for operation planning, radio therapy or diagnostics, and studying the differences of healthy subjects and subjects with tumour. Its major purpose is to split an image into meaningful non-overlapping regions which analysis, interpretation or quantification can be performed [1]. In the past years, a large number of researches have focused on the development of medical image segmentation methods for the reason that accurate segmentation of biomedical images can contribute to simplified diagnosis, surgical planning and prognosis [2].

Detection of abnormalities in brain tissue area in different medical images is inspired by the necessity of high accuracy when dealing with human life. A variety of diseases occur in the brain tissue area such as brain tumour, stroke, infarction, haemorrhage and others. Magnetic Resonance Imaging (MRI) has a proven capability to provide high quality medical images and has been widely used especially in brain. To date, brain diseases are detected by imaging only after the appearance of neurological or nervous system symptoms. Schmidt *et al.*

Shafaf Ibrahim is with the Faculty of Computer and Mathematical Sciences, University Technology MARA, 40150 Shah Alam MALAYSIA e-mail: shafaf_ibrahim@yahoo.com.

Noor Elaiza Abdul Khalid and Mazani Manaf are with the Faculty of Computer and Mathematical Sciences, University Technology MARA, 40150 Shah Alam MALAYSIA.

[3] stated that no early brain diseases detection strategies can diagnoses individuals that are at risk. Nishimura *et al.* [4] claimed that brain diseases are not easily detected by radiologist and neurologist caused by the similar texture of brain abnormalities which leads to the difficulties during the differential diagnosis. Consequently, radiologist and neurologist used an invasive method by injecting some kind of contrast medium for detecting brain abnormalities [5].

Gross tumour volume (GTV) is defined as the area of visible tumour or areas deemed to contain tumour. Presently, GTV borderlines are manually segmented on the medical images by clinicians [6]. This is a long and painful task [7] and furthermore this method is unreliable and error sensitive [8, 9]. These problems consequently affect the accuracy of the target volume of irradiation. High speed computing machines on the other hand enable the observation of the volume and location of the abnormalities visually [10].

There are various segmentation techniques in medical imaging depending on the region of interest [11]. In recent years, medical image segmentation problems has been approached with several solution methods by different range of applicability such as Particle Swarm Optimization [12], Genetic Algorithm [13], Adaptive Network-based Fuzzy Inference System (ANFIS) [14], Region Growing [15]-[17], Active Contour Snake model [15], Self Organizing Map (SOM) [18] and Fuzzy c-Means (FCM) [19]. However, segmenting the brain internal structures remains a challenging task due to their small size, partial volume effects, anatomical variability and the lack of clearly defined edges [20]. Thus, considerable effort is required in order to find reliable and accurate algorithms to solve this difficult problem. The most relevant ones for our problem are SBRG [17], ANFIS [14] and FCM [19] segmentation methods. As it showed some potential, the techniques had been tested in brain abnormalities which produced encouraging results.

SBRG is a region-based technique that controlled by a number of initial seeds [21]. From the initial seeds, it tries to find connected regions with the same property which produces an accurate segmentation. This architecture is very attractive especially for semantic object extraction as well as image applications. In medical field, SBRG algorithm is observed to be successfully implemented as a segmentation technique of medical images [22]-[25].

Fuzzy logics and neural networks are two corresponding technologies. Fuzzy rule-based models are easy to understand because it uses if-then rules structure and linguistic terms.

Conversely, the understanding of neural networks knowledge has been difficult since it learns from data and feedback [26]. The hybrid technique of neural networks and fuzzy logic has produced a new technique of neuro-fuzzy system called Adaptive Network-based Fuzzy Inference System (ANFIS) [27]. The implementations of ANFIS in biomedical engineering have been reported to be very effective in various applications such as automatic control, data classification, decision analysis, computer vision [28] as well as medical [29]-[32]. The ANFIS was claimed to be very effective due to its sensitivity and ability of making uncertainty decisions especially in medical applications [30].

The FCM on the other hand represents a clustering-based method which attempts to classify a voxel to its class using the notion of similarity properties [33]. More specifically, it is a workable soft computing methodology that has been successfully applied in a number of discipline scientific areas such as modeling [34], decision making [35], pattern recognition and classification [36], segmentation [37] as well as medical application areas [38]. In the medical application area, FCM is successfully used to model and analyze the medical process, decision-making [39], [40], image segmentation [37] and tumour grading [41]-[43].

Therefore, this paper compares the performances of SBRG, ANFIS and FCM techniques by determining the patterns and characteristics for various types of brain tissues. This can be used to segment abnormalities in the human brain in order to identify any existence of brain abnormalities. The basic concept is that the local textures in the images can reveal the characteristic of abnormalities of the biological structures. The accuracy of the segmentation results are then compared with the results obtained by each technique.

The organization of the rest of this paper is as follows: Section II presents our methods, including the overview of methodology and descriptions of SBRG, ANFIS and FCM algorithms structure. Section III discusses our results and discussions. Finally, we present our conclusion in Section IV.

II. METHODS

SBRG, ANFIS and FCM are applied for segmenting the abnormalities that occur in the brain tissue areas of MRI brain images. The key concept in this segmentation algorithm is the analysis of texture statistics which are used to find the minimum, maximum and mean value of grey level pixels. It is used as the objective function in all three methods. It is done by extracting the region of interest (ROI) from the MRI brain images in order to identify the patterns and characteristics of each part in brain tissue area. Subsequently, SBRG, ANFIS and FCM techniques will be applied respectively to segment the abnormality objects from the other brain tissue matters of a MRI brain image.

A. Data Collection

Hundred and twenty axial slices of Fluid Attenuated Inversion Recovery (FLAIR) sequence brain MRI of normal and abnormal patients are acquired for the testing purposes. The MRI brain images are obtained from adult male and female

skulls (age range between 20 to 60 years) from the Department of Diagnostic Imaging, Hospital Kuala Lumpur (HKL).

B. Data Analysis

Texture statistics refers to the classification of normal and abnormal brain tissue patterns or texture. Region of interest (ROI) are extracted from the MRI brain images for distinguishing the patterns and characteristics of each part in brain tissue area shown in Fig. 1.

The ROI are divided into four categories of brain component which are:

- 1) Ventricle
- 2) Membrane
- 3) Dark Abnormality
- 4) Light Abnormality

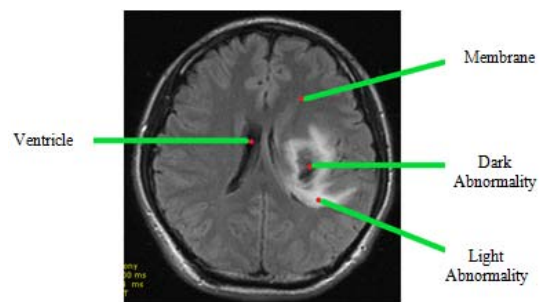


Fig. 1. Proposed brain ROI

Fifty seven ROI data of the four brain component categories had been taken from the MRI images. The ROI image pattern and characteristics are determined by the MinGL, MaxGL and MeanGL as explained in Table I and a summary of the results is shown in Table II.

TABLE I
PARAMETERS FOR BRAIN TISSUE ANALYSIS

Parameter	Description
MinGL	Minimum grey level pixel value occurred
MaxGL	Maximum grey level pixel value occurred
MeanGL	Mean of grey level pixel value occurred

TABLE II
SUMMARY OF REFERENCE TABLE

Brain Component	MinGL	MaxGL	MeanGL
Ventricles	69-108	99-131	86-115
Membrane	7-55	35-92	14-66
Dark Abnormality	6-53	45-118	22-83
Light Abnormality	115-186	161-216	139-199

C. Algorithm Design and Prototype Construction

The main process of segmenting abnormalities in a particular MRI brain image is performed during this stage. The techniques of SBRG, ANFIS and FCM are proposed.

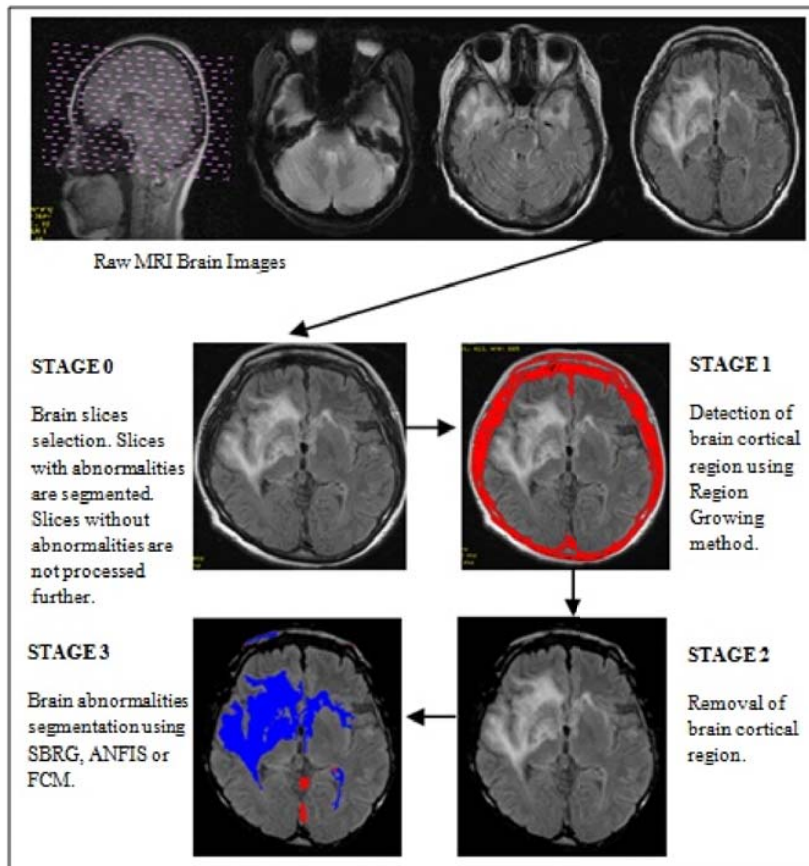


Fig. 2. Proposed brain abnormalities segmentation algorithm

As depicted in Fig. 2, four main stages of the proposed brain abnormalities segmentation algorithm are described in the following section.

1) Stage 0: Brain slice selection

A pre-processing stage in image acquisition works is used to select the brain slices that contain abnormalities. Slices that are free from abnormalities are not processed further

2) Stage 1: Detection of brain cortical region

Detects the region of brain cortical using Region growing technique.

3) Stage 2: Removal of brain cortical region

Removes brain cortical region detected by Stage 1 previously. Regions found to be brain cortical are removed, with those regions remaining labeled as membrane area.

4) Stage 3: Segmentation of abnormalities

Implements SBRG, ANFIS and FCM techniques for segmentation of abnormalities respectively. Completes the abnormalities segmentation by segmenting the region of abnormalities detected.


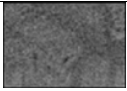
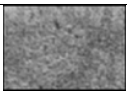
D. Result Analysis

The results for this study are evaluated using a method called accuracy check. A total of 120 images, including the

57 images testing images are known to contain abnormalities.

The experiment in this paper uses three types of normal brain tissue intensities background as shown in Table III.

TABLE III
BACKGROUND IMAGES

Background	Intensity	Minimum pixel value	Maximum pixel value	No. of pixels
	Low	30	114	12144
	Medium	39	145	12144
	High	56	202	12144

Different shaped ROI of light and dark abnormality are cut and pasted onto the background as tabulated in Table IV. This is used to test out the performance and accuracy of the SBRG, ANFIS and FCM segmentation.

Two methods of analysis are employed to quantify the

TABLE IV
SAMPLES OF TESTING IMAGES

Background Abnormality	High	Medium	Low
Light			
Dark			

segmentation accuracy of each technique proposed which are Receiver Operating Characteristic (ROC) analysis and Pearsons correlation. ROC analysis is a plot of the true positive fraction versus the true negative fraction that produced by classifying each data point as positive and negative according to outcome [44]. It has been effectively used as a statistical validation tools in various areas of segmentation such as mammograms [45], retinal [46], brain [47] and skin [48].

In this paper, the numbers of pixels of the raw MRI brain testing images are compared with the segmented abnormality area. ROC is used to measure the value of false positive, false negative, true positive and true negative. The sample of four conditions areas of false positive, false negative, true positive and true negative during the segmentation are illustrates in Fig. 3.

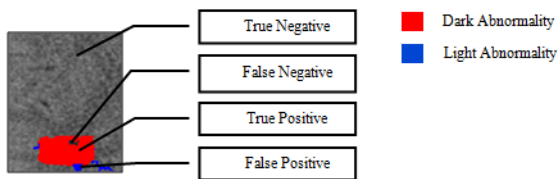


Fig. 3. Sample of testing image of dark abnormality within medium background grey level value after segmentation

The four primary conditions are used to identify the SBRG, ANFIS and FCM segmentation qualities and the level of accuracies for dark and light abnormalities respectively. The descriptions and states for each condition are explained in Table V. The calculations and equations for each condition are represented in (1), (2), (3) and (4).

The second analysis method employed is Pearsons correlation. Pearsons correlation is widely used to reflect the degree of linear relationship between two variables [49]. In this paper, the Pearson correlation value of three categories between the original abnormalities area versus SBRG, the original abnormalities area versus ANFIS, and the original versus FCM segmentation pixels value are measured using (5) so that the variation of results obtained can be clearly monitored.

$$r = \frac{\sum XY - \frac{\sum X \sum Y}{N}}{\sqrt{(\sum X^2 - \frac{(\sum X)^2}{N})(\sum Y^2 - \frac{(\sum Y)^2}{N})}} \quad (5)$$

E. Seed-Based Region Growing (SBRG) Algorithm

Kayvan and Robert [50] discovered that Region growing is an approach to image segmentation in which neighboring pixels are examined and added to a region class if no edges are detected. This process is repeated for each boundary pixel in the region. When any adjacent regions found, a region merging algorithm is used whereby the weak edges are dissolved, while the strong edges are ignored. Fan *et al.* [51] in their paper argued that some region growing methods use the edge as a growth stopping condition where the growing seeds are selected manually. The growth occurs in the homogenous intensity regions and stops at the edges. The segmentation is considered as inaccurate if the edges are broken [51], [52]. Some examples of common region growing techniques include the seed-based, iterative and split and merge [53].

The proposed Region growing algorithm for this paper is the Seed-Based Region Growing (SBRG) as implemented in [25], [54]. It starts by selecting a seed pixel which is located within the abnormality area. Seed pixels are often chosen near to the center of the region as illustrated in Fig. 4.

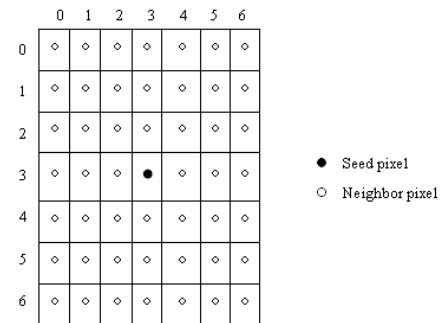


Fig. 4. Location of seed pixel and its 7x7 neighbourhood

The growing process will produce a single region containing pixels with similar properties as the seed pixel. The application of this SBRG algorithm comprises a specification of two variables which are window sized and the absolute difference of grey level value between the grown regions with the seed pixel. Based on the results produced, the window size is chosen to be 3x3 pixels and the absolute grey level threshold is set to 10.

The mean value for the MxM neighborhood is calculated using (6) and the seed expands the region based on a criterion that is defined to determine the similarity between pixels of the region.

$$Mean = \frac{\sum Grey\ level\ pixels\ value\ in\ M \times M\ neighborhood}{\sum No.\ of\ pixels\ in\ M \times M\ neighborhood} \quad (6)$$

There are three possible ways for the seed pixel to grow which are towards its four adjacent neighbors, four diagonal neighbors and eight surrounding neighbors. Fig. 5, Fig. 6 and Fig. 7 show the pictorial representations of each way mentioned.

TABLE V
PRIMARY CONDITIONS OF ROC ANALYSIS

Calculation	State	State	Description
$\frac{\text{segmented area} - \text{abnormality area}}{\text{background size in pixel} - \text{abnormality area}} \quad (1)$	If segmented area > abnormality area	False Positive	the normal areas that are incorrectly detected as abnormality
0	If segmented area \leq abnormality area		
0	If segmented area \geq abnormality area	False Negative	the abnormality areas that are not detected
$\frac{\text{abnormality area} - \text{segmented area}}{\text{abnormality area}} \quad (2)$	If segmented area < abnormality area		
1	If segmented area \geq abnormality area	True Positive	the abnormality areas that are correctly detected
$1 - \frac{\text{abnormality area} - \text{segmented area}}{\text{abnormality area}} \quad (3)$	If segmented area < abnormality area		
$1 - \frac{\text{abnormality area} - \text{segmented area}}{\text{background size in pixels} - \text{abnormality area}} \quad (4)$	If segmented area > abnormality area	True Negative	the normal areas that are correctly undetected
1	If segmented area \leq abnormality area		

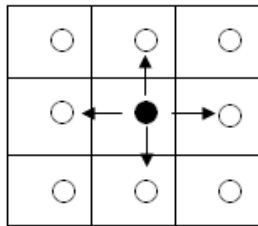


Fig. 5. The 4 adjacent neighbours growth

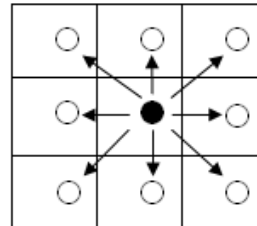


Fig. 7. The 8 surrounding neighbours growth

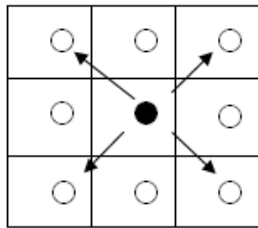


Fig. 6. The 4 diagonal neighbours growth

The algorithm decides the similarity of the neighboring pixels to the other points in the region starting from the seed point. For every growth from the seed pixel to one of its neighbor, the calculated mean value and the grey level of the particular neighbor is compared using (7). If the absolute difference of the two pixels is less than a pre-defined threshold, the neighbor pixel will be included into the growing region.

$$|G_i - M| < T \quad (7)$$

where

G_i = grey level of the particular neighbor pixel

M = calculated mean value of the SBRG

T = pre-defined threshold

The mean value for the region needs to be updated for every inclusion of a neighbor pixel into the region. The growing process is repeated iteratively until all the points are considered.

F. Adaptive Network-Based Inference System (ANFIS) Algorithm

A detail reviews of the ANFIS model has been given in [55], [56]. A neural-fuzzy system is a hybrid of neural networks and fuzzy systems in such a way that neural networks or neural networks algorithms are used to determine parameters of fuzzy system. The main intention of neural-fuzzy approach is to improve a fuzzy system automatically by means of neural network methods. ANFIS is basically has five layer architectures as shown in Fig. 8.

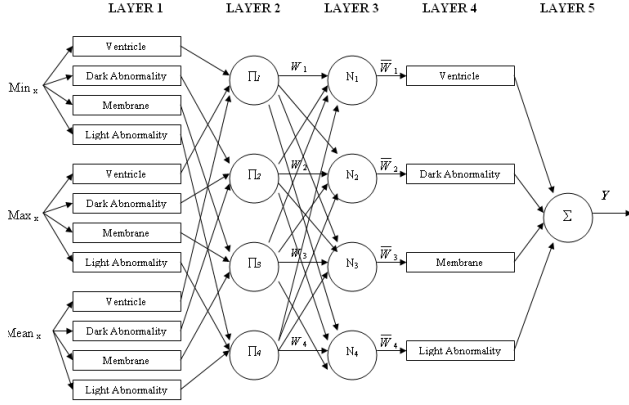


Fig. 8. Proposed ANFIS Architecture

In the first layer, all the nodes are adaptive nodes. The outputs of layer 1 are the fuzzy membership grade of the inputs, which are calculated using (8):

$$o_i^1 = \pi A_i(x) \quad (8)$$

Where x is the input to node i and A_i is a linguistic label such as minimum, maximum and mean grey level value associated with the node. O_i^1 is the membership function of A_i and it specifies the degree to which the given x satisfies the quantifier A_i . $\pi A_i(x)$ is triangle-shaped Membership Function (MF) value ranging from 0 to 1 such as (9):

$$\pi A_i(x) = \frac{1}{1 + (x - c_i/a_i)^{2b_i}} \quad (9)$$

In the second layer, the nodes are fixed nodes. Each node in this layer represents firing strength of the rules. They are labeled with π , indicating that perform as a simple multiplier. The outputs of this layer can be represented as (10):

$$o_i^2 = \pi A_i(x_1) \times \pi B_i(x_2) \times \pi C_i(x_3) \dots \quad (10)$$

where

$i = 1, 2, 3 \dots n$

$x_1, x_2, x_3 \dots n = \text{input}$

$o_i^2 = \text{output of neuron } i$

In the third layer, the nodes are also fixed nodes labeled by N , to indicate that they play a normalization role to the firing strength from the previous layer. The output of this layer can be represented as (11):

$$o_i^3 = \bar{w}_i = \frac{w_i}{w_1 + w_2 + w_3 + w_4} \quad (11)$$

In the forth layer, the nodes are adaptive. The output of each node in this layer is simply the product of the normalized firing

strength and a first order polynomial. Thus, the output of this layer is given by (12):

$$o_i^4 = \bar{w}_i f_i = \bar{w}_i (p_i x_1 + q_i x_2 + r_i x_3 + s_i) \quad (12)$$

Where \bar{w}_i is the output of layer 3 and p_i, q_i and r_i are the parameter set. Parameter in this layer will be referred to as consequent parameters.

In fifth layer, the single layer node is a circle node labeled Σ that computes the overall output as the summation of all incoming signal as (13):

$$o_i^5 = \sum \bar{w}_i f_i \quad (13)$$

G. Fuzzy c-Means (FCM) Algorithm

FCM is an iterative algorithm that aims to find cluster centers in an image that minimizes an objective function. A process called as fuzzy partitioning is employed which a data point can belong to all groups with different membership grades between 0 and 1 [57]. The objective function is the sum of squares distance between each pixel and the cluster centers and is weighted by its membership. FCM is defined by six parameters which are shown in Table VI.

TABLE VI
PARAMETER FOR FCM ALGORITHM

Parameters	Description
n	number of data samples for whole images
c	number of clusters
x_k	k_{th} data sample (pixel point value)
v	i_{th} cluster center
m	weighting exponent (constant greater than unity)
μ	membership of x_k in i_{th} cluster

Step 1: Initialize the constants c, m and ϵ such that:

$$1 \leq c \leq n$$

$$1 \leq m \leq \infty$$

$$\epsilon \leq 0 \text{ a small positive constant}$$

Step 2: Initialize the cluster centers:

$$V_0 = (v_{1,0}, v_{2,0} \dots v_{c,0}) \in R^{CP}$$

For our FCM implementation, the image was clustered into two, which represent abnormality and background based on features values. The algorithm starts by initializing cluster centers to a random value at first time. The performance depends on the initial clusters, thereby allowing running FCM several times, each starting with a different set of initial clusters.

Step 3: Update the membership values using (14):

$$u_{ki} = \frac{1}{\sum_{j=1}^c \left(\frac{\|x_k - v_i\|}{\|x_k - v_j\|} \right)^{2/(m-1)}} \quad (14)$$

Different values of m may produce different segmentation results. Based on literature, the value $m = 2$ was used, to get good performance of FCM.

Step 4: Update the cluster centers using (15):

$$v_i = \frac{\sum_{k=1}^n (\mu_{ik})^m x_k}{\sum_{k=1}^n \sum (\mu_{ik})^m} \quad (15)$$

Step 5: Check terminating condition using (16):

$$\text{Let } E_t = \sum_{i=1}^n \|v_{i,t} - v_{i,t-1}\|^2 \quad (16)$$

III. RESULTS AND DISCUSSION

The numbers of pixels of the raw MRI brain testing images are compared with the SBRG, ANFIS and FCM abnormalities segmented area. Then, every percentage value of false positive, false negative, true positive and true negative are measured by relating the results to any certain circumstances. The samples of MRI brain testing images segmentation outcomes for SBRG, ANFIS and FCM are tabulated in Table VII.

Table VIII tabulates the summary of Receiver Operating Characteristic (ROC) analysis for SBRG segmentation results. The statistical values obtained are used to quantify the SBRG segmentation quality and the level of accuracy for dark and light abnormality in three different types of background which are high, medium and low background grey level value.

TABLE VIII
SUMMARY OF ROC ANALYSIS FOR SBRG

Abnormality	B/Ground Grey Level Value	Mean of False Positive	Mean of False Negative	Mean of True Positive	Mean of True Negative
Light	High	0.335	0.041	0.959	0.665
	Medium	0.011	0.042	0.958	0.999
	Low	0	0.086	0.914	1
Dark	High	0	0.144	0.856	1
	Medium	0.010	0.100	0.900	0.990
	Low	0.032	0.132	0.868	0.968

SBRG shows the most excellent segmentation results in the medium background grey level values for light abnormality as it produced the highest mean percentages for both true positive and true negative. This proved that the SBRG segmentation results showed some potential as the mean percentage of false positive and false negative are kept at a very low rate too. The combination of light abnormality within the low background grey level value also cannot be underestimated even though a small occurrence of mean percentage of false negative is observed. The combination of light abnormality within the high background grey level value is seen to produce

poor performance as it appears to possess the highest mean percentage of false positive.

In contrast, dark abnormality shows good segmentation prospective in the medium background grey level value too. The mean percentage of false negative appears to have increased in the combination of dark abnormality within the low background grey level value. Same goes for the combination of dark abnormality within the high background grey level value as it produces the highest mean percentage of false negative compared to the medium and low background grey level value.

Alternatively, Table IX illustrates the ROC table for ANFIS results analysis summary include the same primary conditions as SBRG too.

TABLE IX
SUMMARY OF ROC ANALYSIS FOR ANFIS

Abnormality	B/Ground Grey Level Value	Mean of False Positive	Mean of False Negative	Mean of True Positive	Mean of True Negative
Light	High	0.532	0	1	0.468
	Medium	0.006	0.006	0.994	0.994
	Low	0	0.027	0.973	1
Dark	High	0.578	0.055	0.945	0.422
	Medium	0.004	0.055	0.945	0.996
	Low	0	0.048	0.952	1

The ANFIS is observed to produce an optimum segmentation of light abnormality in medium background intensity as it produced the highest mean values for both true positive and true negative. The performance of light abnormality segmentation in low background intensity also returns good segmentation outcome as it displays excellent mean value of true negative. However, there is slightly lower in the mean of true positive value since it is affected by the small occurrence of false negative. Same as SBRG, the segmentation of light abnormality within the high background intensity performed unsatisfactorily since it produced the highest mean value of false positive compared to the medium and low background intensity.

For dark abnormality, ANFIS returns the same outcomes as SBRG where it produced a most excellent performance of segmentation in low background intensity since it keeps the mean values for both true positive and true negative at the highest assessment. The combination of dark abnormality within the medium background intensity also cannot be underrated since it produced high mean values for both true positive and true negative. However, small occurrence of false positive and false negative are monitored. The combination of dark abnormality within the high background intensity exhibits poor performance by returning the highest value of false positive.

Conversely, the ROC table for FCM segmentation results analysis summary is tabulated in Table X.

As seen from the Table X, FCM shows the most excellent segmentation result in low background grey level value for light abnormality. The statistics show that the combination produced the highest mean percentages for both true positive and true negative which are the most important conditions in producing good quality of segmentation. In addition to

TABLE VII
SBRG VS ANFIS VS FCM SEGMENTATION

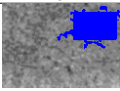
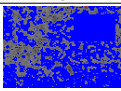
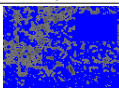
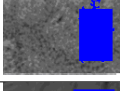
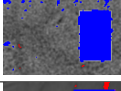
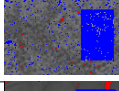



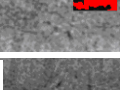
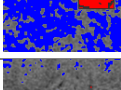
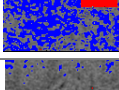
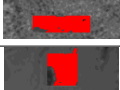
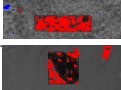
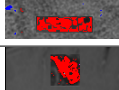



Abnormality	B/Ground	SBRG Segmentation	ANFIS Segmentation	FCM Segmentation
Light	High			
	Medium			
	Low			
Dark	High			
	Medium			
	Low			

TABLE X
SUMMARY OF ROC ANALYSIS FOR FCM

Abnormality	B/Ground Grey Level Value	Mean of False Positive	Mean of False Negative	Mean of True Positive	Mean of True Negative
Light	High	0.469	0	1	0.531
	Medium	0.038	0.001	0.999	0.962
	Low	0	0.011	0.989	1
Dark	High	0.413	0.024	0.976	0.587
	Medium	0.003	0.101	0.899	0.997
	Low	0	0.100	0.900	1

this, the combination of light abnormality within the medium background grey level value cannot also be underestimated since it produces high mean percentages for both true positive and true negative, although a slight value of mean of false positive can be observed. The combination of light abnormality within the high background grey level value gives a poor performance as it appears to have the highest mean percentage of false positive. This is found to be caused by the texture similarity for both light abnormality and high background grey level value that leads to the neighboring pixels expanding to grow beyond the abnormality areas.

On the other hand, dark abnormality shows good segmentation result in low background grey level value as it returns the highest mean percentage of true positive and true negative too. However, the mean percentage of false negative shows moderate significance making the process of segmentation of dark abnormality not as good when compares to the segmentation in the light abnormality areas. The mean percentage of false negative appears to increase in the combination of both dark abnormalities within the medium and high background grey level value. This is caused by confusion of the prototype in

distinguishing the texture similarity between the dark abnormalities with an anatomical brain structure which is ventricles. Therefore, several improvements for the dark abnormalities segmentation may be necessary to produce better quality of segmentation.

Subsequently, the segmentation performances of SBRG, ANFIS and FCM are compared. The Pearsons correlation value is used to reflect the degree of linearity relationship between the two variables. The correlation value for every original versus SBRG segmentation pixels value, original versus ANFIS segmentation pixels value and original versus FCM segmentation pixels value are measured as represented in Table XI.

TABLE XI
PEARSON'S CORRELATION FOR SBRG, ANFIS AND FCM

Abnormality	B/Ground Grey Level Value	Original vs SBRG Correlation	Original vs ANFIS Correlation	Original vs FCM Correlation
Light	High	0.90	0.89	0.93
	Medium	0.99	0.99	0.99
	Low	0.97	0.99	0.51
Dark	High	0.75	0.62	0.85
	Medium	0.86	0.63	0.48
	Low	0.59	0.62	0.56

From the Table XI, it clearly noticed that SBRG, ANFIS and FCM correlation values are almost excellent in light abnormalities segmentation regardless of backgrounds. However, the FCM is monitored to generate considerably low correlation value in low background tissue intensity.

For dark abnormalities, the correlation values of the SBRG, ANFIS and FCM are noted to produce moderate correlation values in all cases. The SBRG and ANFIS are observed to

return the highest correlation values in medium background intensity. Conversely, the FCM shows the best dark abnormalities segmentation in high background tissue intensity. The overall performances proved that the ANFIS returns the best segmentation performances in light abnormalities, whereas the SBRG on the other hand performed well in dark abnormalities segmentation.

Table XII tabulates the samples of SBRG, ANFIS and FCM segmentation of MRI brain images for both light and dark abnormalities.

IV. CONCLUSION

This paper has presented a comparison of segmentation algorithm performances between three techniques of Seed-Based Region Growing (SBRG), Adaptive Network-based Fuzzy Inference System (ANFIS) and Fuzzy c-Means (FCM) paradigms. All three methods are found to be promising for segmentation of light abnormalities. Nevertheless, the segmentation performances of dark abnormalities are observed to produce moderate significances of correlation values in all conditions. These make the segmentation of dark abnormalities is not as good as segmentation in light abnormalities. It may be due to the insensitiveness of the objective function used, setting of parameter values, or deviation of values in data analysis conducted. Several potential improvements are recommended for the future investigation. First, a feature extraction technique could be applied for the recognition of target objects with a homogeneous texture. This is because certain anatomical parts of the brain such as dark abnormality and ventricles could occasionally be confused. The task of integrating the current method of SBRG, ANFIS and FCM with other computer vision architectures could also be proposed in producing better segmentation results in future.

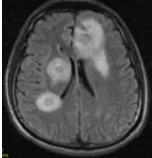
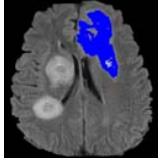
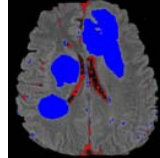
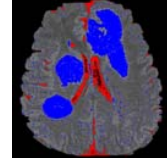
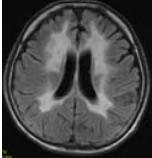
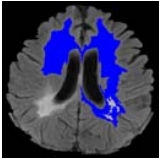
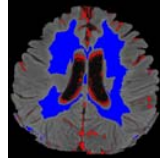
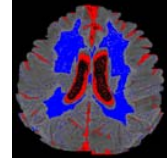
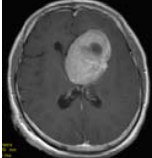
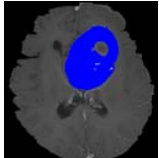
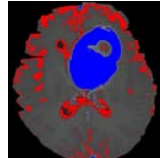
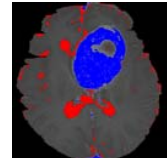
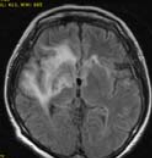
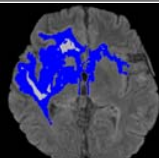
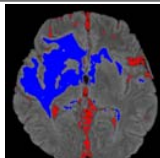
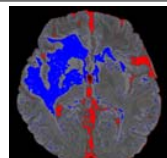
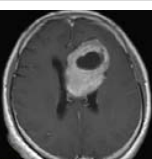
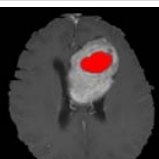
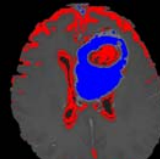
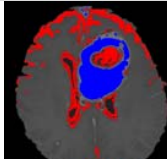
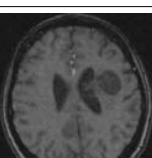
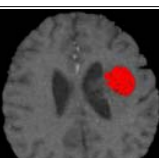
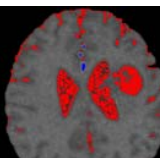
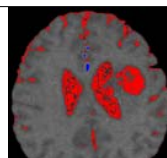
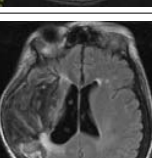
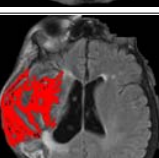
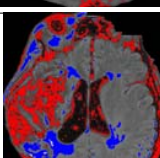
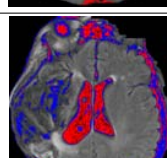
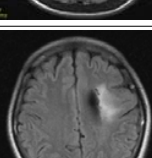
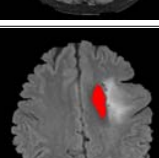
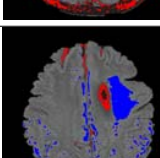
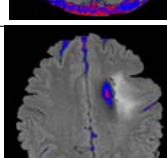
ACKNOWLEDGMENT

The authors would like to thank the Hospital Kuala Lumpur (HKL) for giving their full cooperation during the collection of MRI brain images. Special thanks to the Board Director of HKL, Dr. Hjh Zaleha bt Abdul Manaf the the Head of Radiology (Diagnostic Imaging) Department, and also to all the Diagnostic Imaging staffs.

REFERENCES

- [1] Pal N. R., Pal S. K., A Review on Image Segmentation Techniques, *Pattern Recognition* 26(9), pp. 1277-1294, 1993.
- [2] Nayak H., Amini M. M., Bibalan P. T., Bacon N., Medical Image Segmentation, June 12, 2008.
- [3] Schmidt M., Levner I., Greiner R., Segmenting Brain Tumors using Alignment-based Features. In *Proceedings of the Fourth International Conference on Machine Learning and Applications*, 2008.
- [4] Nishimura A., Sawada S., Ushiyama I., Tanegashima A., Nakagawa T., Ikemoto K., Postmortem Diagnosis of Brain Disorders, *Anil Aggrawal's Internet Journal of Forensic Medicine and Toxicology*, Vol. 1, No. 2, 2000.
- [5] Singh J., Daftary A., Iodinated Contrast Media and Their Adverse Reactions, *Journal of Nuclear Medicine Technology*, Vol. 36, No. 2, pp. 69-74, Society of Nuclear Medicine, Teleradiology Solutions, Bangalore, India, 2008.
- [6] Zizzari A., Udo S., Bernd M., Guenther G., Sebastian S., Detection of Tumour in Digital Images of the Brain, *Proceedings of the IASTED International Conference of the Signal Processing, Pattern Recognition and Application*, Greece, 2001.
- [7] Mancas M., Gosselin B., Macq B., Segmentation Using a Region-Growing Thresholding, *Image Processing: Algorithms and Systems IV*, In: *Proceedings of the SPIE*, Vol. 5672, pp. 388-398, 2005.
- [8] Dong-yong D., Condon B., Hadley D., Rampling R., Teasdale G., Intracranial Deformation Caused by Brain Tumors: Assessment of 3-D Surface by Magnetic Resonance Imaging, *IEEE Transactions on Medical Imaging*, Vol. 12, Issue 4, pp. 693-702, 1993.
- [9] Bouix S., Martin-Fernandez M., Ungar L., Nakamura M., Koo M., McCarley R., Shenton M., On Evaluating Brain Tissue Classifiers without a Ground Truth, *Neuroimage* 07, 447458, 2007.
- [10] Masroor M. A., Dzulkifli M., Segmentation of Brain MR Images for Tumour Extraction by Combining Kmeans Clustering and Perona-Malik Anisotropic Diffusion Model, *International Journal of Image Processing*, Vol. 2, Issue 1, 2008.
- [11] Roerdink J., Meijster A., The Watershed Transform: Definitions, Algorithms and Parallelization Strategies, *Fundamenta Informaticae*, pp. 187-228, IOS Press, 2001.
- [12] Ibrahim S., Khalid N. E. A., Manaf M., Empirical Study of Brain Segmentation using Particle Swarm Optimization, *International Conference on Information Retrieval and Knowledge Management*, CAMP10, 2010.
- [13] Ganesan R., Radhakrishnan S., Segmentation of Computed Tomography Brain Images using Genetic Algorithm, *International Journal of Soft Computing Year 2009*, Vol. 4, Issue 4, pp. 157-161, 2009.
- [14] Noor N. M., Khalid N. E. A., Hassan R., Ibrahim S., Yassin I. M., Adaptive Neuro-Fuzzy Inference System for Brain Abnormality Segmentation, *2010 IEEE Control and System Graduate Research Colloquium*, ICSGRC 2010.
- [15] Khalid N. E. A., Ibrahim S., Manaf M., Ngah, U. K., Seed-Based Region Growing Study for Brain Abnormalities Segmentation, *International Symposium on Information Technology 2010 (ITSim 2010)*, 2010.
- [16] Dubey R. B., Hanmandlu M., Gupta S. K., Semi-automatic Segmentation of MRI Brain Tumor, *ICGST-GVIP Journal*, ISSN: 1687-398X, Vol. 9, Issue 4, August 2009.
- [17] Wasserthal C., Engel K., Rink K., Brechman A., Automatic Segmentation of the Cortical Grey and White Matter in MRI using Region Growing Approach based on Anatomical Knowledge, Springer Berlin Heidelberg, ISBN978-3-540-78639-9, 2008.
- [18] Iftekharuddin K. M., Zheng J., Islam M. A., Lanningham F., Brain Tumor Detection in MRI: Technique and Statistical Validation, *Fortieth Asilomar Conference on Signals, Systems and Computers*, Oct. 29 2006-Nov, pp. 1983-1987, 2006.
- [19] Shen S., Snadham W., Granat M., Sterr A., MRI Fuzzy Segmentation of Brain Tissue using Neighborhood Attraction with Neural Network Optimization, *IEEE Transactions on Information Technology in Biomedicine*, Vol. 9, Issue 3, Sept. 2005, pp. 459-467, 2005.
- [20] Linguraru M. G., Ballester M. A. G., Ayache N., Deformable Atlases for the Segmentation of Internal Brain Nuclei in Magnetic Resonance Imaging, *International Journal of Computers, Communications and Control*, 2007(II): pp. 26-36.
- [21] Adams R., Bischof L., Seeded Region Growing, *IEEE Trans. Pattern Anal. Machine Intell.*, Vol. 16, pp. 641-647, 1994.
- [22] Ngah U. K., Ooi T. H., Sulaiman S. N., Venkatachalam, P. A., Embedded Enhancement Image Processing Techniques on A Demarcated Seed Based Grown Region. *Proceedings of Kuala Lumpur International Conference on Biomedical Engineering*, pp. 170-172, 2002.
- [23] Venkatachalam P. A., Ngah U. K., Hani A. F. M., Shakaff A. Y. M., Seed Based Region Growing Technique in Breast Cancer Detection and Embedded Expert System, *Proceedings of International Conference on Artificial Intelligence in Engineering and Technology*, pp. 464-469, 2002.
- [24] Dubey R. B., Hanmandlu M., Gupta S. K., Semi-automatic Segmentation of MRI Brain Tumor, *ICGST-GVIP Journal*, ISSN: 1687-398X, Vol. 9, Issue 4, August 2009, 2009.
- [25] Ooi T. H., Ngah U. K., Khalid N. E. A., Venkatachalam P. A., Mammographic Calcification Clusters Using The Region Growing Technique. *Proceedings of the New Millennium International Conference on Pattern Recognition, Image*, 2000.
- [26] Mancas M., Gosselin B., Macq B., Segmentation using a Region-Growing Thresholding, *Proceedings of the SPIE, Image Processing: Algorithms and Systems IV*, Vol. 5672, pp. 388-398, 2005.
- [27] Yen J., Langari R., Fuzzy logic: Intelligence, Control and Information. Prentice-Hall Inc., pp. 444, 1999.
- [28] *Fuzzy Logic Toolbox, For use with Matlab*, users guide, Version 2, pp. 220, The MathWorks, Inc., 2005.
- [29] Yu S., Guan L., A CAD System for the Automatic Detection of Clustered Microcalcification in Digitized Mammogram Films, *IEEE Transactions on Medical Imaging*, 19, pp. 115-126, 2000.

TABLE XII
SAMPLES OF SBRG, ANFIS AND FCM SEGMENTATION

Abnormality	MRI Brain Images	SBRG Segmentation	ANFIS Segmentation	FCM Segmentation
Light				
				
				
				
Dark				
				
				
				

- [30] Belal S. Y., Taktak A. F. G., Nevill A. J., Spencer S. A., Roden D., Bevan S., Automatic Detection of Distorted Plethysmogram Pulses in Neonates and Pediatric Patients using an Adaptive-Network Based Fuzzy Inference System. *Artificial Intelligence in Medicine*, 24, pp. 149-165, 2002.
- [31] Ubeyli E. D., Guler I., Automatic Detection of Erythematous Diseases using Adaptive Neuro-Fuzzy Inference Systems, *Computers in Biology and Medicine*, 35, pp. 421-433, 2005.
- [32] Ubeyli E. D., Guler I., Adaptive Neuro-Fuzzy Inference Systems for Analysis of Internal Carotid Arterial Doppler Signals, *Comput Biol Med*, 2005, in press.
- [33] Stylios C. D., Groumpos P. P., Fuzzy Cognitive Maps in Modeling Supervisory Control Systems, *Journal of Intelligent Fuzzy System* 8, pp. 83-98, 2000.
- [34] Miao Y., Liu Z., On Causal Inference in Fuzzy Cognitive Maps, *IEEE Trans. Fuzzy Syst.* 8, pp. 107-119, 2000.
- [35] Liu Z., Satur R., Contextual Fuzzy Cognitive Map for Decision Support In Geographic Information Systems, *IEEE Trans. Fuzzy Syst.* 5, pp. 495-507, 1999.
- [36] Chang X., Li W., Farrell J., A C-means Clustering Based Fuzzy Modeling Method, *The Ninth IEEE International Conference on Fuzzy Systems*, Vol.2, pp. 937-940, BIME Journal, Vol. 06, Issue 1, Dec. 2006.
- [37] Kannan S. R., Segmentation of MRI using New Unsupervised Fuzzy C Mean Algorithm, *ICGST International Journal on Graphics, Vision and Image Processing*, Vol.05, No.2, pp.17-23, January, 2005.
- [38] Murugavalli S. Rajamani V., A High Speed Parallel Fuzzy C-Mean Algorithm for Brain Tumor Segmentation, *BIME Journal*, Volume 6, Issue 1, pp. 29-34, Dec., 2006.
- [39] Papageorgiou E.I., Stylios C.D., Groumpos P.P., An Integrated Two-Level Hierarchical Decision Making System Based on Fuzzy Cognitive Maps, *IEEE Trans. Biomed. Eng.* 50 (12), pp. 1326-1339, 2003.
- [40] Liew AWC, Yan H., An Adaptive Spatial Fuzzy Clustering Algorithm for MR Image Segmentation, *IEEE Trans. Med. Imag.* 2003; 22(9): pp. 1063-75.
- [41] Papageorgiou E.I., Spyridonos P. Ravazoula P., Stylios C. D., Groumpos P. P., Nikiforidis G., Advanced Soft Computing Diagnosis Method for Tumor Grading, *Artif. Intell. Med.* 36 (1), pp. 59-70, 2006.
- [42] Chuang K. S., Tzeng H. L., Chen S., Wu J., Chen T. J., Fuzzy c-means clustering with spatial information for image segmentation, *Computerized Medical Imaging and Graphics*, 30: pp. 9-15, 2006.
- [43] Spyridonos P., Papageorgiou E. I., Groumpos P. P., Nikiforidis G., Integration of Expert Systems with Image Analysis Techniques for Medical Diagnosis, In: *Proc ICIAR 2006, Lecture Notes in Computer Science*, Vol. 4142, Springer-Verlag, pp. 110-121, 2006.
- [44] Gribskov M., Robinson N. L., Use of Receiver Operating Characteristic (ROC) Analysis to Evaluate Sequence Matching *Comput. Chem.*, Vol. 20(1), pp. 25-33, 1996.
- [45] Qian W., Li L., Clarke L. P., Image Feature Extraction for Mass Detection In Digital Mammography: Influence of Wavelet Analysis, *The International Journal of Medical Physics Research and Practice*, Vol. 26, Issue 3, 1999.
- [46] Joao V. B. S., Jorge J. G. L., Roberto M. C. Jr., Herbert F. J., Michael J. C., Retinal Vessel Segmentation Using the 2-D Morlet Wavelet and Supervised Classification, *Journal of IEEE Trans Medical Imaging*, Vol. 25, no. 9, pp. 1214-1222, Sep. 2006.
- [47] Budde M. D., Kim J. H., Liang H. F., Schmidt R. E., Russell J. H., Cross A. H., Song S. K., Toward Accurate Diagnosis of White Matter Pathology using Diffusion Tensor Imaging, *Journal of Magnetic Resonance in Medicine*, Vol. 57, Issue 4, pp. 688-695, April 2007.
- [48] Sigal L., Sclaroff S., Athitsos V., Skin Color-Based Video Segmentation under Time-Varying Illumination, *IEEE Transactions on Pattern Analysis and Machine Intelligence*, Vol. 26, Issue 7, pp. 862-877, July 2004.
- [49] Trochim W., *The Research Methods Knowledge Base*, 2nd Edition. Atomic Dog Publishing, 2000, Cincinnati, OH.
- [50] Kayvan N., Robert S., *Biomedical Signal and Image Processing*, Published by CRC Press, ISBN 0849320992, 2006.
- [51] Fan S. L. X., Man Z., Samur R., Edge Based Region Growing - A New Image Segmentation Method, *Proceedings of the ACM SIGGRAPH International Conference on Virtual Reality Continuum and its Applications in Industry*, pp. 302-305, ISBN:1-58113-884-9, 2004.
- [52] Le-Mair, M. W., Reeves, A. P., Region Growing on a Hypercube Multiprocessor, *Proceedings of the Third Conference on Hypercube Concurrent Computers and Applications*, Vol. 2, Pasadena, California, United States, pp. 1033-1042, ISBN:0-89791-278-0, 1989.
- [53] Hai O. T., Ngah U. K., Khalid N. E. A., Venkatachalam P. A., Region Growing Techniques on Breast Ultrasound Images, *Proceedings of the New Millennium International Conference on Pattern Recognition, Image Processing and Robot Vision (PRIPROV)*, 2000.
- [54] Mat-Isa N. A., Mashor M. Y., Othman N. H., Seeded Region Growing Features Extraction Algorithm; Its Potential Use in Improving Screening for Cervical Cancer, *International Journal of The Computer, the Internet and Management*, Vol. 13(1), pp 61-70, January-April 2005.
- [55] Jang J. S. R., Sun C. T., Mizutani E., *Neurofuzzy and soft computing. A Computational Approach to Learning and Machine Intelligent*. United States of America. Prentice Hall International, 1997
- [56] Nauck D., Klawonn F., Kruse R., *Foundations of Neuro-Fuzzy Systems*. England. John Wiley & Sons Ltd, 1997.
- [57] Albayrak S., Fatih Amasyal F., Fuzzy c-Means Clustering on Medical Diagnostic Systems, *International XII. Turkish Symposium on Artificial Intelligence and Neural Networks (TAINN)*, 2003.



Shafaf Ibrahim is a third semester student of PhD in Science in University Technology MARA, Shah Alam, Malaysia. She holds a Master in Computer Science (2009) and a Bachelors Degree of Computer Science (2007), all from University Technology MARA. Her research interest covers Image Processing, Medical Imaging, Computer Vision, Artificial Intelligence and Swarm Intelligence.



Noor Elaiza Abdul Khalid is a lecturer in University Technology MARA, Shah Alam, Malaysia. She holds a PhD in Computer Science (2010) from University Technology MARA, a Master in Computer Science (1992) from University of Wales and a Bachelors Degree of Computer Science (1995) from University Science Malaysia. Her research interests are Swarm Intelligence, Evolutionary Computing algorithms, Fuzzy and Medical Imaging.



Mazani Manaf is a lecturer in University Technology MARA, Shah Alam, Malaysia. He holds respected position at Faculty of Computer Science and Mathematics as Deputy Dean (Student & Alumni), with various professional and community activities and program assessor. His research interest covers Image Processing, Pattern Recognition & Machine Intelligent and Mobile & Distributed Computing.